Journal of Applied Fluid Mechanics, Vol. 11, No. 4, pp. 1125-1131, 2018.
Available online at www.jafmonline.net, ISSN 1735-3572, EISSN 1735-3645.
DOI: 10.29252/jafm.11.04.27928

Comparative Flow Field Analysis of Boundary Layer Diverter Intake and Diverterless Supersonic Intake Configuration

I. Arif†, S. Salamat, M. Ahmed, F. Qureshi and S. Shah

Department of Aerospace Engineering, College of Aeronautical Engineering, National University of Sciences and Technology, H-12, Islamabad, Pakistan

†*Corresponding Author Email: arsalan_sayani@cae.nust.edu.pk*

(Received April 30, 2017; accepted April 4, 2018)

ABSTRACT

In this paper comparative flow field analysis of two intake configuration i.e. Boundary Layer Diverter Intake and Diverterless Supersonic Intake is carried out based on dimensionless parameters under various flow conditions. Numerical analysis of aircraft intake is a complex phenomenon which involves both external and internal flow analysis. In this research, both external and internal flow characteristics of intake duct are analyzed in detail. A comprehensive mesh scheme is devised and implemented to accurately capture the flow behavior in external surrounding of intake duct and flow passing through the intake duct. The analysis is carried out at different flow conditions to analyze the flow behavior in subsonic and supersonic regimes. Engine design mass flow rate is used for accurate intake analysis and results are validated with available literature. Boundary layer diversion and pressure recovery are examined for each intake configuration and comparative analysis based on pressure recovery is carried out subsequently. The analysis reveals that at subsonic and transonic regimes, Boundary Layer Diverter intake is much more effective than Diverter less Supersonic Intake, however, in supersonic regime Diverter less Supersonic Intake is found be to more effective. The research can further help in modifying/ improving the design of an existing intake configuration for enhanced intake efficiency.

Keywords: Aerodynamics; Boundary layer Diverter intake; Diverterless supersonic intake; Pressure recovery.

NOMENCLATURE

α	angle of attack	P_R	pressure recovery
DSI	Diverterless Supersonic Inlet	ρ_∞	density
BLD	Boundary Layer Diverter	P	static pressure
CFD	Computational Fluid Dynamics	*S-A*	one equation Spalart-Allmaras turbulence model
M #	Mach number	*RANS*	Reynolds Averaged Navier-Stokes
v	velocity	*y+*	non-dimensional length scale associated with turbulence model

1. INTRODUCTION

For a fighter aircraft the design of intake is one of the very important factors. Intake characteristics directly affects the overall performance of an aircraft (Goldsmith and Seddon 1993). The design of a supersonic aircraft intake is one of the most challenging task due to complex flow characteristics such as diffusion and distortion. Also, the design of intake requires efficient operation over a wide range of flow conditions (Paul, Kuppa *et al*. 2011). The intake must be able to deliver required engine flow rate, minimize pressure loss, drag and distortion (Sudhakar and Ananthkrishnan 1996, Taskinoglu and Knight 2002). Over the years Diverterless supersonic intake has gained significant importance due to its simplicity, stealth characteristics and effectiveness (Kim 2009). Diverterless Supersonic Inlet (DSI) has an added advantage of delivering required mass flow rates as compared to clean intake. The parent theory behind the design of bump in DSI is based on Wave rider concept (Goldsmith and Seddon

1993). In boundary layer diverter intake configuration, diverter separates the inlet from the fuselage and the boundary layer. This design feature not only causes added intake weight and drag, but maintenance requirements are also increased (Mattingly 2002). This intake type is successfully designed and tested on F-16 aircraft (Frant and Kozakiewicz 2011). Both intake configurations have their own characteristics based on the engine requirements and aircraft required maneuverability as shown in Fig. 1.

Fig. 1. Boundary layer diverter intake (left) and diverterless supersonic intake (right)

During CFD analysis of aircraft, intakes are often simplified due to complexities involved in flow properties and involvement of both external and internal flow dynamics. However, this simplification usually affects the computed results. This limitation necessitates the integration of internal flow with external flow during CFD analysis (Tu, Yeoh *et al.* 2012).

Although both intake configurations are associated with certain pros and cons, but it is important to assess their performance quantitatively at similar conditions. However, not much literature can be found in this area due to complexities involved in numerical analysis of intakes and assessing their performance with different configurations. Hence, great potential in literature exists in this field of research. For this purpose, dimensionless parameter such as pressure recovery is selected for comparative analysis of intake performance on existing aircraft configuration.

For intake analysis, generally, only the forward fuselage area of aircraft is modeled, therefore, same strategy is adopted in this research as well. Numerical analysis is performed at different flow speeds with varying angle of attack (AoA), zero side slip angle and design mass flow rate. Validation of the results is carried out with available literature on the subject (Mattingly 2002, Ibrahim 2008). In the later part of this research, a comparative analysis is performed with an aircraft having Diverterless Supersonic Aircraft based on dimensionless parameters at similar flow conditions (Hassan, Masud *et al.* 2015). The proposed methodology in this research is aimed to contribute in the research gap that exists in current literature as far as comparative qualitative assessment of intake configurations are concerned.

2. GEOMETRY AND MODELING

For this research, one of the most challenging task was to develop/modify CAD geometry of aircraft with intake configuration under study. The geometrical model of aircraft with Boundary Layer Diverter intake (Config 1) was already available at Numerical Analysis Lab of the Institute. However, the acquired model had number of additional features which were not required for this research and were removed such as external stores, wing attachments, landing gears, landing gear doors, antennas, exhaust nozzle and weapons etc. Due to symmetry of aircraft in longitudinal axis, only right half of the model was used which resulted in optimal utilization of computational resources and time. For further simplicity, only forward fuselage area with intake was used and rear fuselage area including vertical tail, horizontal tail, ventral fin and exhaust nozzle were removed. CAD model of aircraft before and after simplification are shown in Fig. 2.

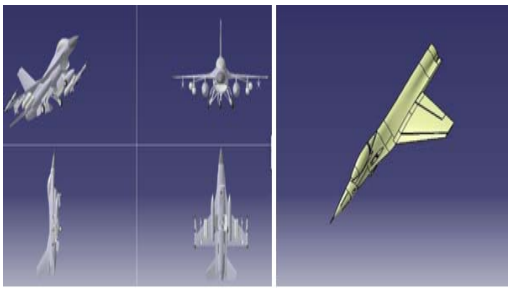

Fig. 2. CAD model before simplification (Left) and after simplification (Right)

3. COMPUTATIONAL SETUP

Computational Fluid Dynamics is a branch of fluid mechanics which use basic conservation laws for numerical simulation. ANSYS® FLUENT solver works on the principle of control volume approach. For numerical analysis in this study, Reynolds-averaged Navier-Stokes (RANS) set of equations are used to account for time dependent behavior of flow. RANS helps in optimum utilization of computational resources by averaging the flow quantities over the entire range of turbulence scale. RANS equations also cater for Reynolds stressors that form an important part of flow analysis. The governing conservation equations are:

Conservation of Mass:

$$-\frac{\partial \rho}{\partial t}=\frac{\partial(\rho u)}{\partial x}+\frac{\partial(\rho v)}{\partial y}+\frac{\partial(\rho w)}{\partial z} \tag{1}$$

Conservation of Momentum:

$$\rho\left(\frac{\partial u}{\partial t}+u\frac{\partial u}{\partial x}+v\frac{\partial u}{\partial y}+w\frac{\partial u}{\partial z}\right)=-\frac{\partial p}{\partial x}+\mu\left(\frac{\partial^2 u}{\partial x^2}+\frac{\partial^2 u}{\partial y^2}+\frac{\partial^2 u}{\partial z^2}\right)+F_x \tag{2}$$

$$\rho\left(\frac{\partial v}{\partial t}+u\frac{\partial v}{\partial x}+v\frac{\partial v}{\partial y}+w\frac{\partial v}{\partial z}\right)= -\frac{\partial p}{\partial y}+\mu\left(\frac{\partial^2 v}{\partial x^2}+\frac{\partial^2 v}{\partial y^2}+\frac{\partial^2 v}{\partial z^2}\right)+F_y \quad (3)$$

$$\rho\left(\frac{\partial w}{\partial t}+u\frac{\partial w}{\partial x}+v\frac{\partial w}{\partial y}+w\frac{\partial w}{\partial z}\right)= -\frac{\partial p}{\partial z}+\mu\left(\frac{\partial^2 w}{\partial x^2}+\frac{\partial^2 w}{\partial y^2}+\frac{\partial^2 w}{\partial z^2}\right)+F_z \quad (4)$$

Conservation of Energy:

$$\rho C_p\left(\frac{\partial T}{\partial t}+u\frac{\partial T}{\partial x}+v\frac{\partial T}{\partial y}+w\frac{\partial T}{\partial z}\right)=\Phi + \frac{\partial}{\partial x}\left[k\frac{\partial T}{\partial x}\right]+\frac{\partial}{\partial y}\left[k\frac{\partial T}{\partial y}\right]+\frac{\partial}{\partial z}\left[k\frac{\partial T}{\partial z}\right] \quad (5)$$

where,

ρ is the fluid density; μ is the kinematic viscosity; u,v,w are the component of velocity in Cartesian coordinates; p is the pressure term; Fx, Fy, Fz are the body force terms; T is temperature in Kelvins; and k is the heat transfer coefficient.

The numerical approach employed in the current study is based on the study carried out by Hassan *et al.* , so that validation of results can be carried out at the later stages of this research. For numerical analysis, modeled geometry of aircraft with intake duct was imported in ANSYS ICEM CFD ® for mesh generation. Semi spherical domain was made around the aircraft and symmetry plane was used in longitudinal axis. Mesh consistency was given prime importance for both types of intakes / configurations to conduct comparative analysis at a later stage in this research. Unstructured meshing scheme was used for both geometries in this research. This step was followed by numerical simulations in Fluent® software. Analysis was carried out at different flow conditions to analyze the flow behavior and intake performance in subsonic and supersonic regime. Simulations were carried out at zero side slip angle and various angle of attack. Flow characteristics such as boundary layer diversion and pressure recovery are examined for each configuration. For comparative analysis of both types of intakes pressure recovery values were compared.

3.1 Grid Generation

Grid generation is one of the most important factors in numerical simulation. A number of public domain and commercial mesh generation softwares are available. For this research, ANSYS ICEM CFD® was used for meshing, as it is industry standard and can produce high quality hexa and hybrid meshes. A very fine mesh could be computationally expensive (Liu, Pekkan *et al.* 2004). Hence, in this work, a crafted grid was used, where in mesh was kept fine at critical areas such as intake cowl lip, intake duct, and fuselage cone etc. In order to ensure mesh consistency, same mesh strategy was adopted for both the geometries (Hassan, Masud *et al.* 2015). Domain size was kept 20 times the fuselage diameter to accurately model flight conditions away and in near vicinity of aircraft without the influence of far field (Masud and Akram 2011). For surface meshing, 'all tri mesh' technique with Patch independent method is used in this work. For volume meshing Robust Octree method was used. This method actually generates the volume by making layers of the surface mesh. Turbulent y^+ values were kept at optimum level for subsonic and supersonic speeds (Tu, Yeoh *et al.* 2012). A size function was also applied to gradually coarsen the mesh size away from the aircraft as shown in Fig. 3.

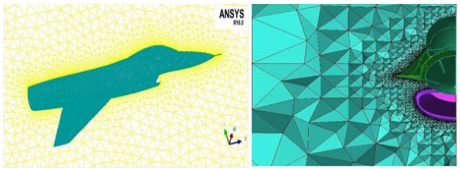

Fig. 3. Volume mesh (left) and cut plane view of volume mesh (right)

3.2 Grid Independence

The accuracy of results in numerical analysis largely depends upon the grid structure and mesh size. A very fine mesh can produce good results but can be computationally expensive and hence it can result in much larger computational time to achieve the desired results. Therefore, a balance must be maintained between the mesh size and accuracy of results. For said purpose, a grid independence test was carried out in order to select an optimized mesh size which produce accurate results and is computationally suitable as well. Four different meshes were generated based on number of cells. All four meshes were generated with different surface mesh size and size function. Pressure Recovery at M # 0.6 and AoA 0^0 for each mesh was evaluated for comparative analysis. A brief summary is also presented in following Table 1 and results are shown in Fig. 4.

rsonic1. Grid independence analysis

Grid	Cells
Grid 1	4.1 million
Grid 2	8.3 million
Grid 3	10.2 million
Grid 4	12.4 million

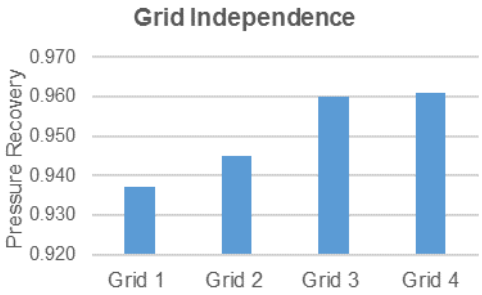

Fig. 4. Grid independence

From Grid independence study, it was observed that values of Pressure Recovery were almost identical

for Grid 3 (10.2 million) and Grid 4 (12.4 million), whereas for Grid 1 and Grid 2, the values of Pressure Recovery varied significantly. Based on these results, a Grid size of 10.2 million cells was selected for accurate results and optimum computational efficiency.

3.3 Boundary Conditions

Aircraft and intake geometries were created separately. These were required to be imported in ANSYS Fluent for numerical analysis. Firstly, meshed aircraft geometry and domain were imported in Fluent and subsequently intake duct, having the same global coordinates, was also imported using 'append' command. The common face of aircraft and intake duct geometries was defined as 'interface'. 'Pressure outlet' condition was used at engine inlet plane to control the engine mass flow rate. Aircraft surfaces were treated as wall with no slip condition. Flow conditions were controlled by changing M # and Angle of attack (AoA) with Pressure Far Field boundary condition at the domain surfaces. Symmetry plane was defined as Symmetry boundary condition. Air is used as ideal gas throughout the analysis.

3.4 Analysis Strategy

Numerical analysis is based on Reynolds-Averaged Navier-Stokes (RANS) equations to predict the flow behavior with time dependency. Density based solver was chosen for present research and explicit technique was implemented in Fluent. Flow discretization was selected as '2nd order upwind', whereas '1st order upwind' scheme was used for turbulent viscosity (Hassan, Masud *et al.* 2015). Default Relaxation parameters were modified to stabilize the iterative process. Courant number, for density based explicit solver, was set at its default value of "1". To ensure the stability of the solution, Aircraft and 'intake duct' were initially simulated separately in Fluent. Once the individual solution were stabilized, two geometries (aircraft and 'intake duct') were integrated using 'append' feature in Fluent, and a combined case was simulated and results were obtained after attaining pre-defined convergence criterion.

3.5 Turbulence Model Independence

Turbulence Model selection also affects the accuracy of numerical solution obtained from CFD significantly, and hence careful selection of same cannot be overlooked. For the purpose of this study, three different turbulence models were selected (SA. k-epsilon and k-omega) based on the fact that the primary physical phenomenon to be captured is flow inside intake duct. SA is a single equation turbulence model while k-epsilon and k-omega are two equation turbulence models. Comparative results for these models are presented in Fig. 5 below:

It was observed that except Standard k-epsilon, all other models (SA and K-omega) were consistent in calculated Pressure Recovery. In addition to this, it was also observed that K-omega model convergence was also a matter of concern as its results depicted a sinusoidal behavior and did not converge at a single value. Hence, its final value was obtained by averaging the values of last 500

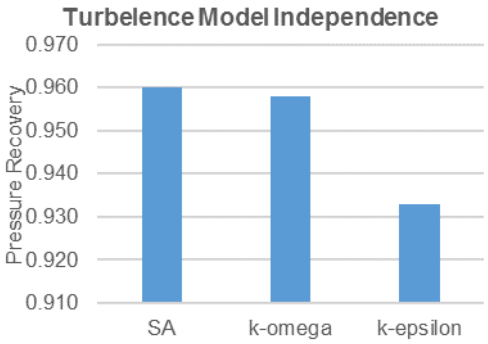

Fig. 5. Turbulence model independence

iterations. Also, its residuals remained above 1x10-4, whereas all other models had their residuals well below 1x10-6 and depicted better convergence rates. Based on these results, SA turbulence model was selected for further analysis. Also, Spalart-Allmaras (S-A) model is specially designed for aerospace applications involving wall-bounded flows, as was the case in this research (Spalart and Allmaras 1992). This RANS model solves transport equation for modified eddy viscosity, and is therefore, not only computation less intensive, but, the in the modified form, eddy viscosity is easy to resolve near the wall. A single solution took an average time of three days to stabilize on a high-end work station (sixteen core CPU with 32 Gigabytes of RAM).

4. RESULTS AND DISCUSSION

In the present study, simulations was carried at two subsonic flight conditions (M # 0.6 and 0.8) and one supersonic flight condition (M # 1.5). Furthermore, at each M #, two AoA (0º and 4º) were analyzed. Therefore, a total of six simulations were performed. All cases were performed at engine design mass flow rate for each condition and no sideslip angles. Flow behavior was analyzed qualitatively and compared for both intake configurations. Qualitative analysis reveals flow entrainment pattern into the intake and thus better intake configuration can be decided. Later, intake performance is calculated in the form of pressure recovery and comparative analysis is carried out between both Config 1 and Config 2 for detailed study.

4.1 Configuration 1- Boundary Layer Diverter (BLD) Intake

F-16 aircraft intake has a significant advantage due to location (under belly) with splitter plate which provides shielding and avoids boundary layer suction at different flight regimes as shown in Fig. 6. The intake shape and curvature to F-16 duct has a direct effect on pressure recovery.

Flow field characteristics of Config 1 are presented in detail. To analyze the flow behavior inside the intake duct, planes were made inside the duct and

total pressure contours are plotted on these plane using post processing tools in Fluent. The total pressure contours plots at M # 0.6, 0.8 and 1.5 are shown in Fig. 7 below.

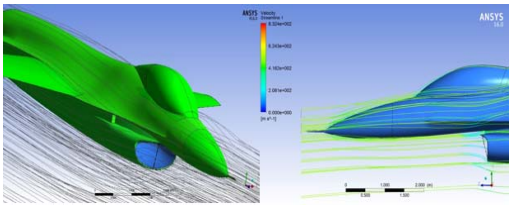

Fig. 6. Velocity streamlines

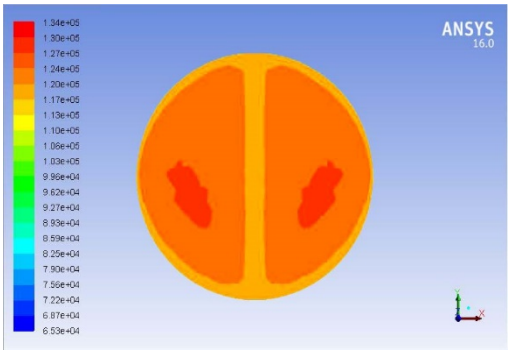

Fig. 7a. Pressure contour at intake duct exit plane at M # 0.6, AoA=0^0

Fig. 7b. Pressure contour at Intake duct exit plane at M # 0.8, AoA=0^0

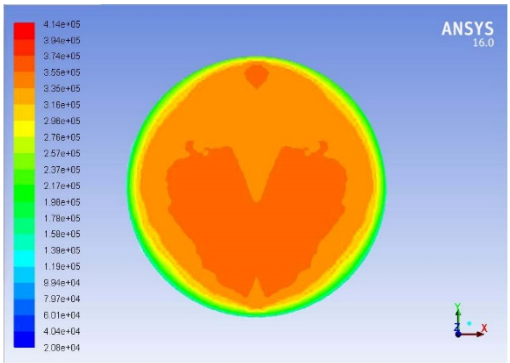

Fig. 7c. Pressure contour at intake duct exit plane at M # 1.5, AoA=0^0

From the figures, it is evident that the flow is largely affected by the duct geometry. The low boundary layer flow does not disperse quickly due to static pressure gradients and results in vortex formation. At M # 0.8 and 1.5, twin swirl flow is prominent at outlet plane due to symmetric nature of intake duct. It was observed that centerline curvature had a direct effect on flow as compared to cross sectional dimensions. The characteristics of boundary layer in the direction of duct was directly affected by local pressure changes. At the sharp curvature of duct, the kinetic energy of flow becomes high and results in large centrifugal forces. Hence, the major cause of secondary flow is due to pressure gradients involved. Low pressure region is visible at duct plane edges at M # 1.5. With increase in angle of attack from 0 degree to 4 degrees, it can be observed that high pressure region is slightly diffused. The high pressure region is evident at the centre of plane and slightly diffuses towards the edges. The fuselage area before intake duct causes the growth in low total pressure area at lower side of intake and causes the velocity to decrease. In all cases, with an increase in AoA, the twin swirls strength decreases which exhibit the optimum design feature of fuselage as flow straightener.

The performance of aircraft intake is usually gauged in terms of pressure recovery, which is the ratio of total pressure at engine inlet to the free stream total pressure. Intakes are designed maximize the pressure recovery and great efforts have been made to minimize the pressure loss due to friction, shock waves and shock boundary layer interaction (Whitford 1987, Mattingly 2002). Since pressure recovery is a dimensionless parameter, it was feasible to perform the comparative analysis based on this parameter. The values of total pressure were extracted from Fluent software at required areas at different flow conditions. Comparative analysis was performed at three different M # and two AoAs at engine mass flow rate. The calculated values of pressure recovery for Config 1 are shown in Table 2 and Table 3.

Table 2 Pressure recovery at AoA 0^0

M #	P_∞ (Pa)	P_{engine} (Pa)	P_{engine} / P_∞
0.6	129240	123888	0.960
0.8	154453	150790	0.976
1.5	371967	349649	0.940

Table 3 Pressure recovery at AoA 4^0

M #	P_∞ (Pa)	P_{engine} (Pa)	P_{engine} / P_∞
0.6	129240	124281	0.961
0.8	154453	149482.6	0.967
1.5	371967	345431	0.928

From the calculated results, it can be observed that at a particular AoA, as the velocity is increased in subsonic regime pressure recovery is increased. Therefore pressure recovery is highest at M # 0.8 at same AoA. Pressure recovery tends to decrease at supersonic speed at all conditions. This is due to the fact that the shock waves at the inlet in supersonic condition causes additional pressure loss and hence it results in lower pressure recovery as compared (Goldsmith and Seddon 1993, Mattingly 2002). This phenomena is quite similar in fixed intakes (Ibrahim, Ng *et al*. 2011). It is also evident that the pressure recovery of BLD (Config 1) is quite

similar for both AoA at M # 0.6, however, at high subsonic and supersonic speeds pressure recovery at AOA 0º is slightly higher than that at AOA 4º. This is due to the fact that the high velocity core moves towards the bottom half of the intake exit plane with the increase in AoA. Also, with the increase in AoA, the flow distortion and instability have pronounced effect on total pressure (Saha, Singh *et al*. 2007). The variation in pressure recovery at varying M # for different AoA are shown in Fig. 8. The average percentage difference in pressure recovery at high subsonic and supersonic speeds at AoA 0^0 and 4^0 is observed to be 1% only.

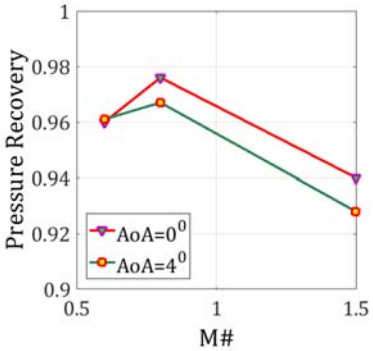

Fig. 8. Pressure recovery vs M #

The results obtained from numerical analysis were validated from available data in literature of same aircraft configuration (Mattingly 2002, Ibrahim 2008). Pressure recovery obtained from CFD analysis and literature are shown in Fig. 9.

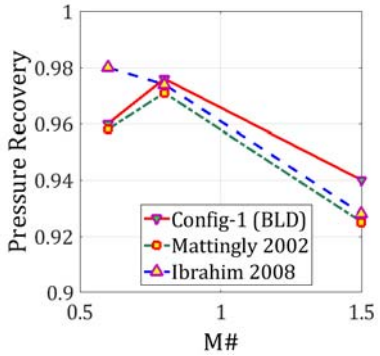

Fig. 9. Pressure recovery comparison

From comparative analysis, it can be observed that the variation in pressure recovery is quite similar except at M # 0.6 of Ref (Ibrahim, 2008) where pressure recovery is high. Also, the pressure recovery calculated in this work is slightly higher than other analysis. This is due to the fact that average design mass flow rate was used for each condition from available literature (Frant and Kozakiewicz 2011) which may differ from the mass flow rate used in other analysis. However, the overall trend line and results are quite satisfactory with available literature.

4.2 Comparative Analysis with Configuration 2 (DSI)

In the next step, a comparative analysis of BLD intake configuration is made with DSI at similar flight conditions and design mass flow rate for each configuration as shown in Fig. 10. Pressure recovery values for Config 2 (DSI) has been published by Hassan *et al.* (Hassan, Masud *et al*. 2015) and same are being used in this research.

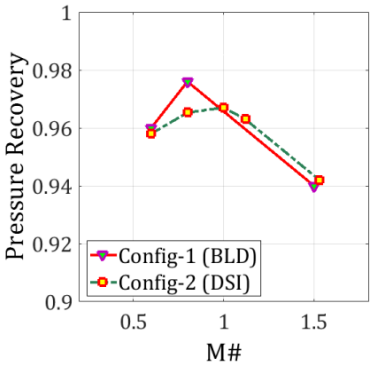

Fig. 10. Pressure recovery comparison of config 1 and 2 at AoA 0^0

From the above graphs, it is evident that both intake configurations have almost same pressure recovery at moderate subsonic speeds of M # 0.6. As the speed increases, in subsonic regime, Config 1 gives better pressure recovery than Config 2. This is due to the fact that boundary layer diverter configuration is quite effective in low subsonic regime due to its shape and location. BLD design prevents ingestion of boundary layer inside the intake and thus increases intake performance. Although, DSI configuration also diverts boundary layer but its effectiveness is less as compared to BLD. As speed is further increased to supersonic speeds, the pressure recovery of both configurations is reduced due to formation of shock waves (Goldsmith and Seddon 1993). In supersonic regime, DSI shows better performance than boundary layer diverter intake in terms of pressure recovery. The pressure downstream of shock wave formed on the bump surface has positive pressure gradient which is responsible for boundary layer diverting away from aircraft intake. At supersonic speed for Config 2, the low energy boundary layer is diverted away from the intake behind the shock wave. Also, at design mass flow rate the oblique shock structure for DSI configuration is similar to design point shock structure which is not observed in BLD configuration. Hence, DSI configuration

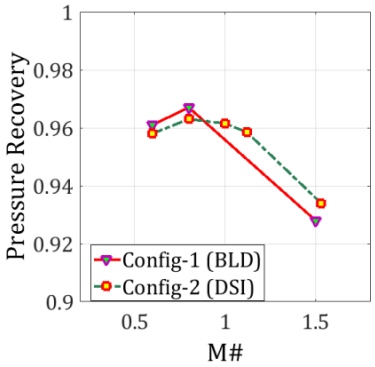

Fig. 11. Pressure recovery comparison of config 1 and 2 at AoA 4^0

has better pressure recovery characteristics than boundary layer diverter intake configuration at high supersonic speeds at design mass flow rate. At AoA

of 4^0, a trend similar to AoA 0^0 is observed, however, there is slight difference in the breakeven point of pressure recovery in both configurations as shown in Fig. 11. Config 2 pressure recovery equals Config 1 pressure recovery at M # 0.9 as compared to M # 1.04 at AoA 0^0 (numerical simulation details not presented in this research). This is due to the fact that the variation in pressure recovery of Config 2 with change in AoA is slightly less than that of Config 1. Hence, DSI performance is less affected by variation in pitching motion of aircraft and maintains optimum mass flow rate for better engine performance.

5. CONCLUSION

In this work flow field and performance analysis of BLD intake configuration is carried out. The results were validated with available literature and a comparative analysis was carried out with an aircraft with DSI configuration. The analysis was carried out at different M # and angle of attack to analyze the flow behavior in subsonic and supersonic regimes. The results revealed that BLD intake configuration is more effective in subsonic regime as compared to DSI configuration, whereas at supersonic speeds DSI configurations gave superior performance. However, it may be noted that the simulations were carried out discretely at zero side slip angle and at a particular height. For complete comparison of the two configurations, more simulations at different numerical setups are under study by the College of Aeronautical Engineering (CAE) research group.

ACKNOWLEDGMENTS

The authors acknowledge the use of Numerical Analysis Lab (NAL) of College of Aeronautical Engineering, Risalpur, Pakistan.

REFERENCES

Frant, M. and A. Kozakiewicz (2011). Construction of an air intake system model for F-100-PW-229 engine in F-16 aircraft for intake vortex development analysis. *Prace Instytutu Lotnictwa*. 39-49.

Goldsmith, E. L. and J. Seddon (1993). Practical intake aerodynamic design, Amer Inst of Aeronautics &.

Hassan, S., J. Masud and O. Khan (2015). Intake and Airframe Characterization through Composite CFD. *AIAA*.

Ibrahim, I., E. Ng and K. Wong (2011). Flight Maneuverability Characteristics of the F-16 CFD and Correlation with its Intake Total Pressure Recovery and Distortion. *Engineering Applications of Computational Fluid Mechanics 5*(2): 223-234.

Ibrahim, I. H. (2008). Fluid flow studies of the F-5E and F-16 inlet ducts.

Kim, S. D. (2009). Aerodynamic design of a supersonic inlet with a parametric bump. *Journal of Aircraft 46*(1): 198-202.

Liu, Y., K. Pekkan, S. C. Jones and A. P. Yoganathan (2004). The effects of different mesh generation methods on computational fluid dynamic analysis and power loss assessment in total cavopulmonary connection. *Journal of Biomechanical Engineering 126*(5): 594-603.

Masud, J. and F. Akram (2011). Flow field and performance analysis of an integrated diverterless supersonic inlet. *Aeronautical Journal 115*(1170): 471.

Mattingly, J. D. (2002). Aircraft engine design, *AIAA*.

Paul, A. R., K. Kuppa, M. S. Yadav and U. Dutta (2011). Flow improvement in rectangular air intake by submerged vortex generators. *Journal of Applied Fluid Mechanics 4*(2): 77-86.

Saha, K., S. Singh and V. Seshadri (2007). *Effect of angle of attack on performance of twin intake duct*. 37th AIAA Fluid Dynamics Conference and Exhibition.

Spalart, P. R. and S. R. Allmaras (1992). A one equation turbulence model for aerodinamic flows. *AIAA journal 94.*

Sudhakar, K. and N. Ananthkrishnan (1996). Jump phenomena in Y-shaped intake ducts. *Journal of aircraft 33*(2): 438-439.

Taskinoglu, E. S. and D. Knight (2002). Numerical analysis of submerged inlets. *AIAA Paper 3147*.

Tu, J., G. H. Yeoh and C. Liu (2012). *Computational fluid dynamics: a practical approach*, Butterworth-Heinemann.

Whitford, R. (1987). Design for air combat, Janes Information Group.